European Journal of Operational Research 310 (2023) 117–132

Contents lists available at ScienceDirect

European Journal of Operational Research

journal homepage: www.elsevier.com/locate/ejor

Production, Manufacturing, Transportation and Logistics

Drones for relief logistics under uncertainty after an earthquake

Okan Dukkanci [a,*], Achim Koberstein [a], Bahar Y. Kara [b]

[a] Faculty of Business Administration and Economics, European University Viadrina, Frankfurt (Oder) 15230, Germany
[b] Department of Industrial Engineering, Bilkent University, Ankara 06800, Turkey

ARTICLE INFO

Article history:
Received 15 September 2021
Accepted 25 February 2023
Available online 3 March 2023

Keywords:
Humanitarian logistics
Relief distribution
Drone delivery
Uncertainty
Stochastic programming

ABSTRACT

This study presents a post-disaster delivery problem called the relief distribution problem using drones under uncertainty, in which critical relief items are distributed to disaster victims gathered at assembly points after a disaster, particularly an earthquake. Because roads may be obstructed by debris after an earthquake, drones can be used as the primary transportation mode. As the impact of an earthquake cannot be easily predicted, the demand and road network uncertainties are considered. Additionally, the objective is to minimize the total unsatisfied demand subject to a time-bound constraint on the deliveries, as well as the range and capacity limitations of drones. A two-stage stochastic programming and its deterministic equivalent problem formulations are presented. The scenario decomposition algorithm is implemented as an exact solution approach. To apply this study to real-life applications, a case study is conducted based on the western (European) side of Istanbul, Turkey. The computational results are used to evaluate the performance of the scenario decomposition algorithm and analyze the value of stochasticity and the expected value of perfect information under different parametric settings. We additionally conduct sensitivity analyses by varying the key parameters of the problem, such as the time-bound and capacities of the drones.

1. Introduction

Technological developments in autonomous vehicles and aviation have facilitated the testing and application of unmanned aerial vehicles (UAVs), which are commonly known as drones, for inspection and monitoring purposes (ReportLinker, 2021) in several fields, including agriculture (Meola, 2021), construction (Balfour Beatty, 2017) and airplanes (Manalo, 2015). Additionally, drones have been used for commercial deliveries for organizations, such as UPS (2017) and Amazon (2022), and applied toward humanitarian and healthcare operations. For instance, DHL was part of a collaboration for healthcare and humanitarian applications, in which medicines were delivered to a remote island in Lake Victoria in East Africa. Owing to poor road infrastructure and difficult terrain in the region, six hours were required to reach the island. Instead, the delivery time was reduced to an average of 40 minutes using drones, and rapid service was ensured in the case of an emergency (DHL, 2018). Additionally, the United Nations International Children's Emergency Fund (UNICEF) implemented several humanitarian projects involving drones. For instance, a potential drone corridor was launched in Malawi, using which drones can deliver small and lightweight supplies, such as medicines, vaccines, and samples for diagnoses, including HIV testing (Unicef, 2017). In another UNICEF project, a child received the world's first drone-delivered vaccine in Vanuatu, which is a country comprising remote and mountainous islands. To increase the number of children vaccinated using drone-delivered vaccines, the government first contracted a commercial drone company to transport vaccines to remote areas in the country (Unicef, 2018). Another drone-delivery operation on humanitarian applications was conducted by a medical product delivery company known as Zipline. In 2016, Zipline started delivering blood in Rwanda using drones, and in April 2019, the company started delivering vaccines, blood, and medicine using drones in Ghana. Additionally, Zipline delivered COVID-19-related medical supplies, such as tests and samples in Rwanda and Ghana (Lewis, 2020) as well as COVID-19 vaccines (Vincent, 2021). In addition to this application, they are currently developing drones that can be deployed in post-disaster delivery operations (Zipline, 2022).

Motivated by the aforementioned real-life applications, in this study, we propose a post-disaster humanitarian application, in which drones execute final deliveries. In this setting, we consider possible earthquakes, which may disrupt the road connections owing to possible debris between the supply points of relief items and assembly areas (gathering points), where affected people gather. Aerial vehicles, such as drones, can be used as the main delivery

* Corresponding author.
E-mail address: dukkanci@europa-uni.de (O. Dukkanci).

https://doi.org/10.1016/j.ejor.2023.02.038
0377-2217/

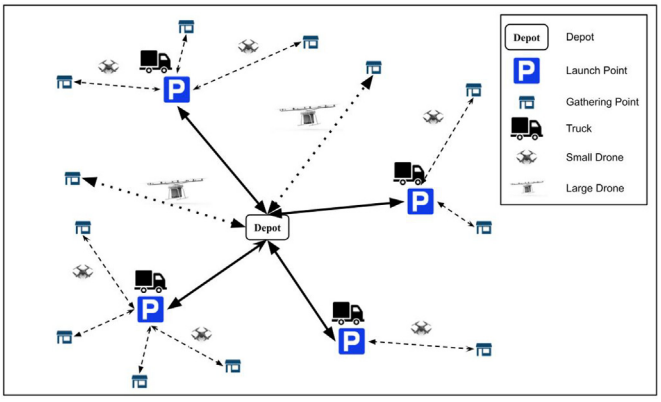

Fig. 1. Proposed drone delivery system.

vehicles to distribute relief items to affected people by minimizing the impact of such an incomplete road network.

In this study, we propose a two-echelon delivery system that uses trucks and two types of drones: large and small. Small drones have a limited payload capacity and range, whereas large drones have a large capacity and range. Trucks operate at the first echelon to transport small drones and relief items from depots to launch points, where the small drones are launched and used to conduct final deliveries to gathering points in the second echelon. By contrast, large drones carry relief items to gathering points directly from their launching depots. Small drones can also make direct deliveries from depots. In this setting, trucks are not allowed to make deliveries to limit truck operations on road as much as possible. Another reason for not using trucks in deliveries is to make sure of fair distribution of relief items since affected people might want to take more than what they might actually need due to the fear of not getting those items in the coming days. Figure 1 displays the delivery system described above with one depot and four launch points (indicated by P). In the figure, the solid arrows represent truck movements between the depot and launch points, dashed arrows represent the deliveries by small drones between the launch points and gathering points, and dotted arrows represent the deliveries by large drones between the depot and gathering points.

Although using drones as delivery vehicles can provide a complete network in the case of an earthquake, drones are generally subject to range and capacity limitations. As a function of the battery capacity and drone speed, the drone range is the maximum distance that a drone travels without recharging. Owing to the importance of time in this setting, we assume that the drone battery is replaced after each return journey, and while the old battery is recharging, the new battery is used for uninterrupted delivery operations. Drone range is an issue specifically for small drones, as large drones have very long ranges. However, capacity restrictions apply to both types of drones and trucks. To ensure that all deliveries are completed within a short duration owing to emergencies, a time-bound constraint is additionally included in this problem.

One of the main reasons for the devastating impact of earthquakes is that they cannot be predicted in advance. In particular, the time, place, and magnitude of earthquakes are unpredictable. Therefore, the number of relief items required by affected people and the effect on the road network cannot be predicted before an earthquake occurs. For that reason, we consider the uncertainties of demand and road networks. To ensure that relief items are delivered to the maximum number of people, the main aim of the problem is to minimize the total unsatisfied demand at all gathering points.

The problem is defined according to the two-echelon delivery system described above, which consists of choosing depots and launch points from a candidate set of sites, assigning launch points to depots, assigning gathering points to launch points to be served by the small drones, and/or depots to be served by large drones. These are subject to the capacity restrictions of the trucks and drones, time-bound assigned for completing all deliveries, and the range of the small drones.

To the best of our knowledge, this is the first study that considers a relief distribution problem under demand and road network uncertainties on a two-echelon network, in which range-limited drones (assisted by trucks) are used to deliver critical items within a predetermined time-bound. The contributions of this study are as follows: (i) we introduce a new post-disaster delivery problem, which features an endogenous drone range and a time-bound, as well as demand and road network uncertainties; (ii) we first present a two-stage stochastic formulation and its deterministic equivalent problem; (iii) we apply a scenario decomposition algorithm to solve the problem within a reasonable time; (iv) we conduct a case study of Istanbul, Turkey, where we present a novel approach to estimate the demand based on different scenarios in terms of location and magnitude of earthquakes; and (v) we present an extensive computational analysis to evaluate the performance of the scenario decomposition algorithm, analyze the values of stochasticity and perfect information, and consider different parametric settings.

The remainder of this paper is organized as follows. Section 2 presents a literature review of related problems. Section 3 describes a mixed-integer linear programming formulation for the deterministic problem and subsequently elaborates on the two-stage stochastic programming formulation, in which the demand and road network uncertainties are considered. Section 4 presents the proposed solution approach; the scenario decomposition algorithm. Section 5 describes the case study and demand and road distance generation based on earthquake scenarios and presents a computational analysis. Finally, Section 6 concludes the study and presents insights and future research directions.

2. Related literature

This section presents a literature review related to relief distribution using drones under uncertainty and analyzes studies in three different categories: (i) delivery problems using drones, (ii) relief distribution problems under uncertainty, and (iii) relief distribution problems using drones with and without uncertainty.

Recent technological developments in the field of UAVs have increased the number of studies that have considered deliveries using drones. Murray & Chu (2015) introduced two cargo delivery problems, in which a truck and a drone conducted last-mile deliveries. The first was known as the flying sidekick traveling salesman problem (FSTSP), in which when a truck reached a customer, a drone launched from the truck to serve another customer and subsequently returned to the truck at the depot or another customer location. The second problem proposed by Murray & Chu (2015) is known as the parallel drone-scheduling traveling salesman problem. In this case, a truck and drones operated separately, such that the truck was routed between customers and the drones performed dedicated deliveries. The objective function of both problems was to minimize the latest arrival time of the truck or drone at the depot. Wang & Sheu (2019) extended the idea proposed in the FSTSP by considering multiple trucks and proposed vehicle routing using drones. The objective was to minimize the total cost, including the fixed cost of the trucks and transportation costs of the trucks and drones. Murray & Raj (2020) presented another extension of the FSTSP, in which multiple drones were used for deliveries to minimize the latest return time of the truck or drones to the depot. Dorling et al. (2017) proposed vehicle routing for

drone delivery. In contrast to the approaches described above, only drones routed between customers performed last-mile deliveries. Additionally, the authors considered two objective functions: minimizing cost, including the cost associated with energy consumption, and minimizing delivery time. Dukkanci et al. (2021) proposed the energy minimizing and range constrained drone delivery problem, in which trucks departed from the depot, to transport drones and packages to a certain location, and subsequently acted as a launching point for drones that conducted last-mile deliveries to customers. The proposed problem minimized the total cost, which consisted of the operational cost of the trucks and costs associated with the energy consumption of drones. Although the aforementioned studies involved delivery by drones, none of the studies investigated drones for the post-disaster application or considered various uncertainties. Additionally, all the studies considered a cost or time-based objective function rather than a demand-coverage-based one, unlike the present study. For further studies on delivery problems using drones, we recommend that readers should refer to Chung et al. (2020); Macrina et al. (2020); Otto et al. (2018), and Li et al. (2021).

Relief distribution problems have been studied in the literature as part of humanitarian logistics. Because of the stochastic nature of disasters, most problems in this field have considered uncertainties. Tofighi et al. (2016) introduced a two-echelon humanitarian logistics network design problem, in which demand, supply, and transportation network uncertainties were considered for the post-disaster application. The problem was developed as a two-stage scenario-based possibilistic-stochastic program. In the first stage, the locations of central warehouses and local distribution centers, as well as inventory levels of relief items, were determined; the second stage determined relief distribution while considering three different objective functions: minimizing the total distribution time, the maximum weighted distribution time for the critical relief items, and the total cost of unused inventories and weighted shortage cost of unsatisfied demands. Noyan et al. (2016) proposed a relief distribution network design problem under demand and transportation network uncertainties to determine the location and capacity of relief distribution points. The authors considered two supply policies based on equity and accessibility. The objective function of the problem was to maximize the expected total accessibility. The problem was modeled as a two-stage stochastic program and solved using a branch-and-cut algorithm based on Benders' decomposition. Noyan & Kahvecioğlu (2018) extended the study by Noyan et al. (2016) by considering a three-echelon relief distribution network that additionally included local distribution centers. The proposed problem was solved using a scenario-decomposition-based branch-and-cut algorithm. Erbeyoğlu & Bilge (2020) studied a robust relief network design problem under demand uncertainty. In this study, the locations of storage and distribution centers, as well as inventory levels of these facilities, were determined to ensure that the correct combination of relief items was supplied within a certain time. The objective function minimized the total cost in the pre-disaster phase, including the fixed cost of opening the facilities, as well as the acquisition and holding costs associated with prepositioned inventories. To solve this problem, the authors proposed a logic-based Benders' decomposition approach. Grass et al. (2020) considered the relief distribution problem arising in disaster management under demand, supply, and transportation network uncertainties. The authors modeled this problem as a two-stage stochastic problem, in which the first stage determined the locations of the facilities and inventory levels and the second stage determined the distribution of relief items. The objective function minimized the total cost, which consisted of the cost of opening the facilities and prepositioning relief items in the first stage, as well as transportation, unused relief items, and unsatisfied demand in the second stage. The authors proposed an accelerated L-shaped method as a solution. Yang et al. (2021) proposed scenario-robust optimization models for the prepositioning of relief items. Instead of using stochastic programming and robust optimization, the authors considered a distribution-free uncertainty set in the proposed problem. The objective function minimized the total cost consisting of the fixed cost of a facility, acquisition cost of relief items, transportation cost, holding cost of unused items, and penalty cost of unsatisfied demand. Yang et al. (2023) presented a distributionally robust model for a multi-period location-allocation problem with resources and capacity levels under uncertainties of demand and resource fulfilment time. The problem minimized the total cost, including the fixed cost of opening and reopening the facilities, cost of delivering basic and emergency resources, penalty and shortage costs owing to unsatisfied demands. The authors developed a branch-and-Benders'-cut algorithm. Although some similarities exist between the relief distribution problem under uncertainty and the problem in the present study, none of the studies considered range-limited vehicles as last-mile delivery vehicles. Additionally, all vehicles in these studies were ground vehicles, which indicates that relief items were distributed via roads; however, roads can be disconnected after a disaster. Using drones to conduct last-mile deliveries can eliminate such problems. Finally, all problems aimed to minimize the total cost function. Although some studies (Grass et al., 2020; Tofighi et al., 2016; Yang et al., 2021; 2023) included the penalty cost of unsatisfied demand as part of the total cost, none of the studies considered a humanitarian perspective to directly minimizing the total unsatisfied demand, unlike the problem in this study. For more studies on relief distribution problems and two-stage stochastic programming in disaster management, we recommend that readers should refer to Anaya-Arenas et al. (2014) and Grass & Fischer (2016), respectively.

Finally, we analyze the studies on relief distribution problems, in which drones were used for final deliveries. Most studies in this field have considered using only drones, which are limited by capacity and range. Because only drones are used for deliveries, these problems considered single-echelon networks. Golabi et al. (2017) studied a stochastic facility location problem under demand and transportation network uncertainties. The problem assumed that individuals, who are uniformly distributed along the edges of the network, travel to the distribution center if the edge is accessible. However, if the edge is inaccessible, drones deliver relief items. The objective was to minimize the aggregate travel time for people (accessible edges) and UAVs (inaccessible edges). Although several uncertainties were considered, the problem proposed a single echelon network, in which only drones were used as delivery vehicles. Rabta et al. (2018) studied a problem, in which drones were allowed to visit recharging stations to extend their range. The authors assumed that the location of the depot and recharging stations were known and the drones can be routed between demand areas. However, they did not consider uncertainty. Kim et al. (2019) studied a stochastic facility location problem, in which the uncertainty of drone operations in terms of flight distance (drone range) was considered. The uncertain flight distance was modeled using chance constraints, instead of considering different scenarios. The objective function minimized the total cost consisting of the fixed cost of opening and operating the facilities, as well as the operational and maintenance costs associated with the drones. Although the problem acknowledged the drone range uncertainty, the drone range limitation was not well addressed, as only drones are used to conduct deliveries. Shavarani (2019) proposed a multilevel facility location problem for relief distribution operations, in which deliveries were conducted by UAVs. The problem can be considered to be an extension of Rabta et al. (2018), as the locations of the launch (supply) points of the drones and recharging stations were determined. However, this study did not address any

uncertainties. Chauhan et al. (2019) presented the maximum coverage capacitated facility location problem with range-constrained drones, in which the locations of the facilities and assignment of drones to the facilities and demand points were determined. The objective function maximized the demand served, and the drone range was calculated as a function of the payload. As this study did not consider uncertainty, Chauhan et al. (2021) extended this problem by considering uncertainties of initial battery availability and consumption in a robust optimization framework. A penalty function associated with the availability of an initial battery was included in the objective function in addition to the demand coverage. Although this problem has a similar objective function to our problem, the range limitation of the drones was insufficiently addressed. Macias et al. (2020) proposed a two-stage sequential optimization approach consisting of a trajectory optimization and location-routing problem. The trajectory optimization was defined as an optimal control problem with a nonlinear formulation to minimize battery consumption. Subsequently, the location-routing problem decided the location of hubs, routes of the drones, and battery management while minimizing the total cost, including the fixed costs of the hubs and batteries, travel time cost, and penalty cost for unsatisfied/over satisfied demand. Gentili et al. (2022) studied a location and scheduling problem, in which drones were launched from platforms for the emergency delivery of perishable items to hard-to-access areas after a disaster. The problem decided the location of the platforms, assignment of the demand points and routes of the drones while minimizing a disutility function depending on the delivery time. The authors also considered a two-period extension of the problem, in which the platforms were relocated in the second period. However, Macias et al. (2020) and Gentili et al. (2022) did not consider uncertainty and assumed that drones can be routed between demand points. Zhu et al. (2022) presented a two-stage robust facility location problem with drones under demand uncertainty. This problem minimized the total cost including the fixed cost of the facilities, transportation cost, and penalty cost of the unsatisfied demand. The authors developed three different optimization models differing in terms of drone energy consumption calculations. The column-and-constraint generation method and Benders' decomposition were used to solve the problem.

A few studies have considered other vehicles such as trucks along drones in relief distribution problem. Fikar et al. (2016) developed a decision support system to optimize the shipments of relief items and simulate disasters. In the proposed problem, off-road vehicles and drones operate together to minimize the average lead time because roads may be blocked. However, the authors did not consider the range limitations of drones, and both vehicles operated separately. Chowdhury et al. (2017) presented a continuous approximation model to supply relief items in a disaster-affected region using drones and trucks, where these two types of vehicles conducted separate deliveries. The model aimed to minimize the total cost, including the total facility cost, total transportation cost of the trucks and drones, and average inventory holding cost of the distribution centers. Additionally, the model decided the locations of the distribution centers, service areas, and ordering quantities of these centers. Jeong et al. (2020) studied the humanitarian flying warehouse problem of delivering relief items to people in conflict zones using drones from an airship. Drones were launched from an airship to serve demand points and subsequently land on a ground station. This study considered a different application and did not consider uncertainty, as well. Faiz et al. (2020) performed the only study that considered using trucks and drones in a relief distribution problem under uncertainty. The authors proposed two variants of the two-echelon vehicle routing problem. The first is a deterministic problem, in which trucks and two types of drones are used. Trucks, which are routed between satellite stations, carry hotspots and delivery drones. After the hotspot drones are routed between demand points to assess the damage for estimating demand, delivery drones are routed between demand points to distribute relief items. The second problem is a stochastic problem, in which trucks and only delivery drones operate under demand uncertainty. A two-stage robust model is developed to solve the latter problem. Although some operational difficulties exist due to impacts of disaster, the authors assumed that the trucks and delivery drones can be routed. Therefore, they focused on a two-echelon vehicle routing problem, instead of a two-echelon facility location problem, unlike this study.

In addition to the distribution of relief items, the literature considered the use of drones in other humanitarian applications, such as search and rescue operations (Kyriakakis et al., 2022) and post-disaster assessment (Zhang et al., 2023).

Table 1 lists the other relief distribution problems using drones, as well as our problem, based on the following factors: (i) the objective function, (ii) the mode(s) of delivery, (iii, iv) whether a parameter or a model was used to define the drone range, (v) whether uncertainty was considered, (vi) whether time bound was included, and (vii) the nature of the solution methods: exact (E) and/or heuristic (H). Compared to the other related problems in the literature, our study proposes a new two-echelon delivery system, in which trucks increase the efficiency of deliveries using range-limited drones. Our problem also includes a different objective function aimed at maximizing the number of people that receive relief items under uncertainty within a predetermined time bound, which has not been considered in any other related studies in the literature.

3. Mathematical formulation

The problem proposed in this study is defined on a complete directed graph $G = (N, A)$, where $N = \{1, \dots, n\}$ is the set of nodes and $A = \{(i, j): i, j \in N, i \neq j\}$ is the set of arcs. Set N of nodes is partitioned by set $D = \{1, \dots, d\}$ of potential depots, set $L = \{1, \dots, l\}$ of potential launch points for small drones, and set $C = \{1, \dots, c\}$ of the gathering points. Additionally, we defined set $U = \{1, \dots, u\}$ of small drones, each with capacity Q_{SD} and preparation time τ. Each gathering point $k \in C$ has a non-negative demand q_k. The capacity and speed of the number of large drones m^{BD} are denoted by Q_{BD} and $v^{BD}_{\max}$, respectively. The flying distance on arc $(i, j) \in A$ is denoted by d^{air}_{ij}, which is assumed to be symmetric, and the driving distance on arc $(i, j) \in A$ is denoted by d_{ij}. The maximum speed limit for small drones is denoted by $v_{\max}$. The (average) speed and capacity of a truck are denoted by $\bar{v}$ and Q_T, respectively. All deliveries must be completed within a given time bound T, and p is the number of depots to be opened and e is the (fixed) number of launch points available for drones to be launched. The maximum speed limit of a small drone that can travel between the gathering point $k \in C$ and launch point $l \in L$ or depot $l \in D$ is denoted by v_{lk}, which is calculated using the range constraint. The total number of small drones is denoted by m^{SD}, which can be calculated by multiplying u and e.

The calculation of the range for small drones is based on the study by Dukkanci et al. (2021), in which the drone range depended on the energy consumption formula (Stolaroff et al., 2018) estimated using the power consumption formula developed by Zeng et al. (2019). The range $R(v)$ (in m) of a drone traveling at a constant speed v (in m/s) is expressed as follows:

$$R(v) = \frac{\Theta}{\frac{\mu_1}{v} + \mu_2 v + \frac{\mu_3}{v^2} + \mu_4 v^2}, \tag{1}$$

where Θ, μ_1, μ_2, μ_3, and μ_4 are constants. More details regarding the calculation of the drone range can be found in Appendix A. We

Table 1
Features of the relief distribution problems using drones .

Reference	Objective	Vehicles	Range		Uncertainty	Time-bound	Method
			Parameter	Model			
Golabi et al. (2017)	Minimize the aggregate traveling time	Drones	✓		✓		H
Rabta et al. (2018)	Minimize the total cost (distance)	Drones		✓			E
Kim et al. (2019)	Minimize the total cost	Drones	✓		✓		H
Shavarani (2019)	Minimize the total distance	Drones	✓				H
Chauhan et al. (2019)	Maximize the demand served	Drones		✓			E & H
Chauhan et al. (2021)	Maximize the demand served and penalty for the initial battery	Drones		✓	✓		E & H
Macias et al. (2020)	Minimize the total cost	Drones		✓			E & H
Gentili et al. (2022)	Minimize a disutility function based on delivery time	Drones	✓				E
Zhu et al. (2022)	Minimize the total cost	Drones		✓	✓		E & H
Fikar et al. (2016)	Minimize average lead time	Drones & Off-road vehicles					E & H
Chowdhury et al. (2017)	Minimize the total cost	Drones & Trucks	✓				H
Jeong et al. (2020)	Maximize the coverage, minimize cost and risk	Drones & Airship		✓			E
Faiz et al. (2020)	Minimize the total cost	Drones & Trucks	✓		✓		E
Our study	Minimize the total unsatisfied demand	Drones & Trucks		✓	✓	✓	E & H

used Eq. (1) to calculate the value of parameter v_{lk} to ensure that the range limitation was satisfied.

Herein, we first present a mixed-integer programming formulation for a deterministic version of the problem. The decision variables are defined as follows: if a candidate site $j \in D$ is operated as a depot, then the binary variable x_j is equal to 1 and 0 otherwise. If a candidate site $l \in L$ is used as a launch point, then the binary variable y_l is equal to 1; otherwise, it is 0. A binary variable w_{lj} equals 1 if the launch point $l \in L$ is assigned to depot $j \in D$ and 0 otherwise. If the gathering point $k \in C$ is supplied by a large drone that launches from a depot $j \in D$, then the binary variable r_{jk} is equal to 1 and 0 otherwise. A binary variable z_{lku} equals 1 if a small drone $u \in U$ launches from a launch point $l \in L$ or depot $l \in D$ to serve the gathering point $k \in C$ and 0 otherwise. Finally, a continuous and nonnegative variable o_k represents the unsatisfied demand for gathering point $k \in C$.

A mathematical formulation for the problem is given as follows:

$$\text{Minimize} \quad \sum_{k \in C} o_k \tag{2}$$

subject to

$$\sum_{j \in D} x_j = p \tag{3}$$

$$\sum_{l \in L} y_l = e \tag{4}$$

$$\sum_{j \in D} w_{lj} = y_l \qquad \forall l \in L \tag{5}$$

$$w_{lj} \le x_j \qquad \forall l \in L, j \in D \tag{6}$$

$$\sum_{j \in D} \sum_{k \in C} r_{jk} \le m^{BD} \tag{7}$$

$$r_{jk} \le x_j \qquad \forall j \in D, k \in C \tag{8}$$

$$\sum_{u \in U} \sum_{k \in C} q_k z_{lku} \le Q_T y_l \qquad \forall l \in L \tag{9}$$

$$q_k - Q_{SD} \sum_{l \in L \cup D} \sum_{u \in U} z_{lku} - Q_{BD} \sum_{j \in D} r_{jk} \le o_k \qquad \forall k \in C \tag{10}$$

$$\sum_{j \in D} \frac{d_{jl}}{\bar{v}} w_{lj} + \sum_{m \in C} \left(\frac{2 d^{air}_{lm}}{v_{lm}} + \tau \right) z_{lmu} \le T \qquad \forall l \in L, u \in U \tag{11.1}$$

$$\sum_{m \in C} \left(\frac{2 d^{air}_{lm}}{v_{lm}} + \tau \right) z_{lmu} \le T \qquad \forall l \in D, u \in U \tag{11.2}$$

$$\frac{d^{air}_{jk}}{v^{BD}_{\max}} r_{jk} \le T \qquad \forall j \in D, k \in C \tag{12}$$

$$x_j \in \{0, 1\} \qquad \forall j \in D \tag{13}$$

$$y_l \in \{0, 1\} \qquad \forall l \in L \tag{14}$$

$$w_{lj} \in \{0, 1\} \qquad \forall l \in L, j \in D \tag{15}$$

$$z_{lku} \in \{0, 1\} \qquad \forall l \in L \cup D, k \in C, u \in U \tag{16}$$

$$r_{jk} \in \{0, 1\} \qquad \forall j \in D, k \in C \tag{17}$$

$$o_k \ge 0 \qquad \forall k \in C. \tag{18}$$

Objective function (2) minimizes the total unsatisfied demand. Constraints (3) and (4) fix the number of depots and launch points to be used for p and e, respectively. Constraints (5) and (6) ensure that each launch point is assigned to a depot that is opened. Constraint (7) ensures that the number of large drones used does not exceed the number of large drones available. Constraint (8) ensures that a large drone will not serve any gathering points from a depot unless the depot is open. Constraint (9) guarantees that a small drone will not launch from a launch point to serve a gathering point unless the launch point is used. Constraint (9) also ensures that the demand for all gathering points assigned to a launch point does not exceed the capacity of the truck at that point. Constraint (10) calculates the unsatisfied demand at each gathering point by subtracting the capacities of the small drones and a large drone assigned to that gathering point from its demand. Constraints (11.1) and (11.2) guarantee that the delivery time of small drones is limited by the given time bound if small drones are launched from launch points or depots, respectively. The first part on the left-hand side of the Constraint (11.1) represents the journey time of the truck from a depot to the launch point. The second part represents the time required for all drone journeys between the truck at a given launch point and all gathering points assigned to it. As Constraint (11.2) only accounts for direct deliveries of small drones from depots, it does not include any truck travel time. Constraint (12) ensures that the time taken for the deliveries made by the large drones is within the given time bound. Constraints (13)–(18) define the variable domains.

3.1. Problem formulation including uncertainty

As mentioned in the problem description, this setting requires the uncertainties of demand and road network. Here, we assume that the demand and road network uncertainties are modeled using a set $S = \{1, \ldots, |S|\}$ of scenarios. Let ξ_k be the random variable representing the demand at gathering point $k \in C$. Next, each gathering point $k \in C$ has a non-negative demand ξ_{ks} with probability p_s for each $s \in S$. Let ω_{lj} be the random variable representing the distance between depot $j \in D$ and launch point $l \in L$. The connection between depot $j \in D$ and launch point $l \in L$ has a non-negative distance ω_{ljs} with probability p_s for each $s \in S$.

The uncertainties of demand and road networks are addressed by first presenting a two-stage stochastic formulation. Therefore, we separate the decision variables into the first and second stages. The depot location x_j, launch point location y_l and assignment of launch points to depots w_{lj} are considered to be the first-stage decisions because these decisions are taken before the realization of the demand and road distance values. The assignment of gathering points to depots r_{jk} and/or to launch points z_{lku} and the unsatisfied demand o_k are considered as second-stage decisions. Therefore, in the two-stage stochastic formulation, they are defined for each scenario $s \in S$, and become r_{jks}, z_{lkus}, and o_{ks}.

$$\text{Minimize} \quad \mathbb{E}\ [Q(x, y, w, \xi, \omega)] \tag{19}$$

subject to

$$\sum_{j \in D} x_j = p \tag{3}$$

$$\sum_{l \in L} y_l = e \tag{4}$$

$$\sum_{j \in D} w_{lj} = y_l \qquad \forall l \in L \tag{5}$$

$$w_{lj} \leq x_j \qquad \forall l \in L, j \in D \tag{6}$$

$$x_j \in \{0, 1\} \qquad \forall j \in D \tag{13}$$

$$y_l \in \{0, 1\} \qquad \forall l \in L \tag{14}$$

$$w_{lj} \in \{0, 1\} \qquad \forall l \in L, j \in D, \tag{15}$$

where $[Q(x, y, w, \xi, \omega)]$ is the optimal value of the second-stage problem, that is,

$$Q(x, y, w, \xi, \omega) = \text{Minimize} \sum_{s \in S} \sum_{k \in C} o_{ks} \tag{20}$$

subject to

$$\sum_{j \in D} \sum_{k \in C} r_{jks} \leq m^{BD} \qquad \forall s \in S \tag{7'}$$

$$r_{jks} \leq x_j \qquad \forall j \in D, k \in C, s \in S \tag{8'}$$

$$\sum_{u \in U} \sum_{k \in C} \xi_{ks} z_{lkus} \leq Q_T y_l \quad \forall l \in L, s \in S \tag{9'}$$

$$\xi_{ks} - Q_{SD} \sum_{l \in L \cup D} \sum_{u \in U} z_{lkus} - Q_{BD} \sum_{j \in D} r_{jks} \leq o_{ks} \quad \forall k \in C, s \in S \tag{10'}$$

$$\sum_{j \in D} \frac{\omega_{ljs}}{\overline{v}} w_{lj} + \sum_{m \in C} \left(\frac{2 d^{air}_{lm}}{v_{lm}} + \tau \right) z_{lmus} \leq T \quad \forall l \in L, u \in U, s \in S \tag{11.1'}$$

$$\sum_{m \in C} \left(\frac{2 d^{air}_{lm}}{v_{lm}} + \tau \right) z_{lmus} \leq T \qquad \forall l \in D, u \in U, s \in S \tag{11.2'}$$

$$\frac{d^{air}_{jk}}{v^{BD}_{jk}} r_{jks} \leq T \qquad \forall j \in D, k \in C, s \in S \tag{12'}$$

$$z_{lkus} \in \{0, 1\} \qquad \forall l \in L \cup D, k \in C, u \in U, s \in S \tag{16'}$$

$$r_{jks} \in \{0, 1\} \qquad \forall j \in D, k \in C, s \in S \tag{17'}$$

$$o_{ks} \geq 0 \qquad \forall k \in C, s \in S. \tag{18'}$$

We assume that the supports of ξ and ω are finite, which indicates that the demand and road distance can take a finite number of values with positive probabilities. According to this assumption, the two-stage stochastic formulation can be represented as a large deterministic problem known as the deterministic equivalent problem (DEP). For each demand point $k \in C$, the random variable ξ_k takes values $\xi_{k1}, \xi_{k2} \ldots, \xi_{k|S|}$, and the random variable ω_{lj} takes values $\omega_{lj1}, \omega_{lj2} \ldots, \omega_{lj|S|}$ with probabilities $p_1, p_2 \ldots, p_{|S|}$ for each scenario $s \in S$. The DEP of the two-stage stochastic programming formulation is given as

$$\text{Minimize} \quad \sum_{s \in S} p_s \sum_{k \in C} o_{ks} \tag{21}$$

subject to

(3)–(6), (7′)–(12′), (13)–(15), *and* (16′)–(18′).

4. Solution approach

Solving the DEP formulation presented in Section 3.1 within a reasonable time does not seem possible, as seen from the results presented in Section 5.3.1. Therefore, we propose an exact solution algorithm to solve the proposed problem, which is based on the scenario decomposition algorithm (SDA) proposed by Ahmed (2013) for two-stage 0–1 stochastic programs where the first-stage decisions are binary. As the problem proposed in this study consists of binary first-stage decision variables, we adapted this algorithm as a solution approach.

The SDA consisted of two phases. In the first phase, the relaxation of the problem is solved, in which the nonanticipativity of the first-stage decision variables is relaxed. This relaxation allows the decomposition of the problem in each scenario. The deterministic problem is solved for each scenario, and a lower bound value is obtained for the main problem using the optimal values of these single-scenario problems. In the second phase of the algorithm, a problem is solved, in which the first-stage decision variables are fixed by the solutions determined in the first phase, and an upper bound is identified for each scenario. Therefore, the upper bound value is obtained for the main problem by considering the expected value of the single-scenario problems.

Additionally, the proposed algorithm does not consider the first-stage variables, which are already evaluated, in the following iterations of the algorithm and identifies tight lower bounds in the first phase. Because the first-stage decision variables are binary, the following constraint can be added to the formulation to eliminate the solutions that have already been evaluated and find a tight lower bound:

$$\sum_{j \in D: \bar{x}_j = 0} \bar{x}_j + \sum_{j \in D: \bar{x}_j = 1} (1 - \bar{x}_j) + \sum_{l \in L: \bar{y}_l = 0} \bar{y}_l + \sum_{l \in L: \bar{y}_l = 1} (1 - \bar{y}_l) + \sum_{l \in L, j \in D: \bar{w}_{lj} = 0} \bar{w}_{lj} + \sum_{l \in L, j \in D: \bar{w}_{lj} = 1} (1 - \bar{w}_{lj}) \geq 1 \quad \forall \{\bar{x}, \bar{y}, \bar{w}\} \in R, \tag{22}$$

where R represents the set of first-stage variable solutions that have already been evaluated.

Algorithm 1 terminates after a finite number of iterations that either result in infeasibility or finding the optimal solution to the problem. If the problem is infeasible for a scenario, UB does not

Algorithm 1 Scenario decomposition algorithm.

initialize: $UB \leftarrow +\infty, LB \leftarrow -\infty, R = \emptyset, x^* \leftarrow 0, y^* \leftarrow 0, w^* \leftarrow 0$

1: **while** $UB > LB$ and $\{0,1\}^{(d+l+dl)} \setminus R \neq \emptyset$ **do**
2: **for** $s = 1$ to S **do**
3: solve the relaxation of the second stage formulation including Constraints (22)
4: let $(\bar{x}_s, \bar{y}_s, \bar{w}_s)$ be the optimal solution and lb_s be the optimal objective value
5: **end for**
6: $LB \leftarrow \sum_{s=1}^{S} p_s lb_s, \hat{R} = \bigcup_{s=1}^{S} \{\bar{x}_s, \bar{y}_s, \bar{w}_s\}, R \leftarrow R \cup \hat{R}$
7: **for** $\{x, y, w\} \in \hat{R}$ **do**
8: $u \leftarrow 0$
9: **for** $s = 1$ to S **do**
10: solve the problem formulation given x, y, and w variables
11: let $f_s(x, y, w)$ be the optimal objective value
12: **if** Problem is infeasible **then**
13: set $f_s(x, y, w) \leftarrow \infty$ and $u \leftarrow \infty$
14: **else**
15: set $u \leftarrow u + p_s f_s(x, y, w)$
16: **end if**
17: **end for**
18: **if** $UB > u$ **then**
19: $UB \leftarrow u$, $x^* \leftarrow x$, $y^* \leftarrow y$ and $w^* \leftarrow w$
20: **end if**
21: **end for**
22: **end while**

take a finite value as $f_s(x, y, w) = \infty$ and $u = \infty$. If the problem is feasible for all scenarios, which indicates that UB takes a finite value, then the algorithm terminates by either exploring all possible first-stage feasible solutions or because the lower bound is greater than or equal to the upper bound ($UB \leq LB$). The algorithm ensures the former termination because the cardinality of $\{0,1\}^{(d+l+dl)} \setminus R$ decreases by at least one in each iteration until the algorithm terminates. Therefore, the algorithm terminates after a maximum of $2^{(d+l+dl)}$ iterations. The algorithm guarantees the latter because the unexplored first-stage solution cannot provide a better objective value than UB, as $UB \leq LB$. Therefore, $\{x^*, y^*, w^*\}$ is the optimal solution to the problem.

To improve the implementation of the decomposition algorithm, we prioritize branching of launch point location variables (y) over depot location (x) and launch point assignment (w) variables for the scenario problems solved in the first phase of the algorithm. Additionally, we apply preprocessing rules in the scenario problems solved in the second phase of the algorithm. The following rules are implemented to reduce the number of second-stage variables: (i) if x_j equals 0 (line 10 of Algorithm 1), then we do not define variables r_{jks} and (ii) if y_l equals 0 (line 10 of Algorithm 1), then we do not define variables z_{lkus}.

5. Computational study

This section presents detailed analyses of the computational experiments conducted in this study. First, we describe the case study and datasets. Second, we explain the calculation of the demand and road distance values based on different earthquake scenarios. Third, we analyze the evaluation of the SDA and the values of stochasticity and perfect information. Finally, we conduct a sensitivity analysis by varying the parameters of the problem.

All mathematical models and algorithms were implemented in Java, and all experiments were conducted in a Windows environment with an AMD Ryzen 9 3950X 16-Core 3.50 gigahertz processor with 128 gigabyte of RAM using Gurobi version 9.0.3 as the solver.

5.1. Dataset

We present an original dataset for post-disaster applications in Istanbul, Turkey. One of the main reasons for choosing Istanbul as a case study is that geological studies and surveys indicate that in the near future, that is, in the next 20 years, a major earthquake is expected to occur there. With a population of approximately 16 million people and irregular urbanization, the impact of such a disaster can be devastating.

The dataset that we consider particularly covers the western (European) part of Istanbul, which consists of 25 districts with approximately 10 million people. This includes 365 schools in total and consists of 329 high schools and 36 university campuses as gathering points, as well as 10 stadiums and large open parking lots as possible launch points for the small drones. Additionally, five candidate depot locations are present. Schools are chosen as gathering points because they contain ample space (schoolyards) for people to gather after an earthquake. Figure 2(a) shows the locations of the gathering points (blue points), launch points for the small drones (yellow Ps), and possible depot locations (orange houses) on the map of Istanbul. In addition to this large dataset, we consider a small dataset consisting of 40 gathering points, seven launch points, and three depots (Fig. 2(b)). The main reason for using the small dataset is to evaluate the performance of the SDA and analyze the value of stochastic optimization and perfect information (Refer to Section 5.3).

5.2. Demand and road distance estimation

Herein, we apply a two-stage approach to estimate the demand at each gathering point and the road distance between each depot and launch point. In the first stage, we use damage intensity level formulae from geological literature to estimate the damage intensity level of a possible earthquake. Subsequently, the estimated level is used to calculate the damage percentages, that is, the number of affected people, based on a past earthquake.

Similar to the approach reported by Noyan et al. (2016), we first calculate the damage intensity levels for possible earthquakes. In the geological literature, several different intensity predictive models were proposed and evaluated for the potential earthquakes in Turkey to calculate the Medvedev Sponheuer Karnik (MSK) scale to determine the damage intensity level (I_s). Noyan et al. (2016) applied the model proposed by Erdik & Eren (1983) specifically for the North Anatolian Fault, where the Istanbul earthquake will potentially occur depending on the surface-wave magnitude (M_s) and epicentral distance (R_{epi}):

$$I_s = 0.34 + 1.54M_s - 1.24 \ln R_{epi} \tag{F1}$$

A recent study by Bayrak et al. (2019) evaluated four intensity predictive models that can be applied to estimate the damage for all potential earthquakes in Turkey. The first two formulae (F2) and (F3) depended only on the magnitude and distance to the fault (epicentral distance), similar to (F1), whereas the other two formulae (F4) and (F5) additionally considered the hypocentral depth (h).

$$I_s = 7.023 + 0.703M_s - 2.826 \log R_{epi} \tag{F2}$$

$$I_s = 5.002 + 0.75M_s - 0.0094R_{epi} - 1.454 \log R_{epi} \tag{F3}$$

$$I_s = 7.494 + 0.744M_s - 3.377 \log \sqrt[3]{R_{epi}^3 + h^3} + 0.017\ h \tag{F4}$$

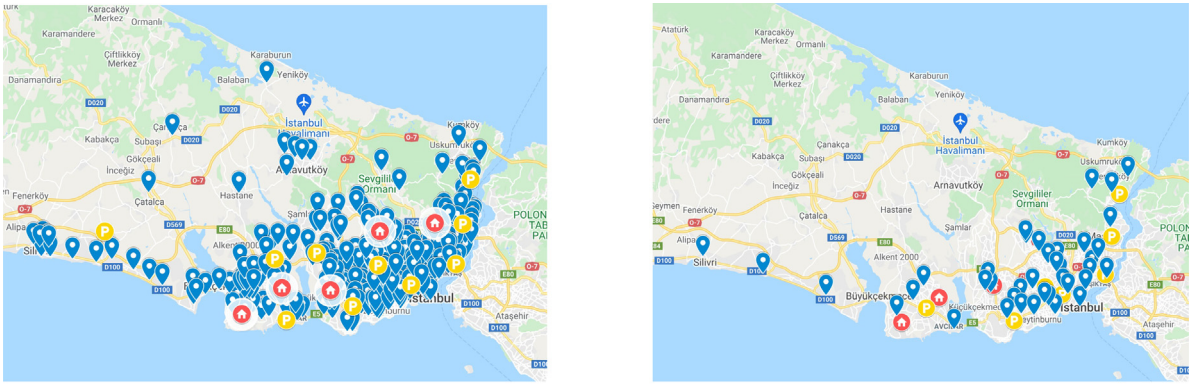

(a) Large dataset (b) Small dataset

Fig. 2. Locations of depots, launch points, and gathering points on the map of Istanbul (Google Maps, 2021).

Fig. 3. Epicenter locations of the earthquakes that occurred in the Marmara Sea in the last ten years (Google Maps, 2021).

$$I_s = 2.281 + 0.874M_s - 0.618\log\sqrt{1+\frac{R_{epi}^2}{h^2}} - 0.016\left(\sqrt{R_{epi}^2+h^2}-h\right) \quad \text{(F5)}$$

Bayrak et al. (2019) did not indicate the best formula among (F2)–(F5) for estimating the damage intensity. However, preliminary analysis revealed that (F1) generally underestimated the damage intensity by approximately one level. This underestimation may be related to the outdated formula (F1), which excludes recent earthquake information. Therefore, we focused on the other four formulae (F2)–(F5) by considering the average values obtained using these formulae while estimating the damage intensity level.

The calculations using the damage intensity formulae require the following information: epicentral distance, hypocentral depth, and magnitude. To calculate the first two, we consider 156 earthquakes that have occurred in the last ten years near Istanbul (Marmara Sea) with magnitudes greater than 3.0 M. Fig. 3 shows the epicenter location of these 156 earthquakes on the map. The earthquake information is available at http://www.koeri.boun.edu.tr/sismo/2/en/. For these earthquakes, we obtained the exact coordinate information of the epicenter and the magnitude and depth information of the earthquake. Here, we consider the use of these coordinates for possible earthquake scenarios. The magnitudes of the earthquakes are then randomly generated using the following uniform distribution: U(6.8, 7.7).

Because we calculated the damage intensity levels of possible earthquakes in the first stage, in the second stage, we estimated the damage percentages. For each intensity level (MSK scale) determined by the average of values obtained using the four formulae (F2)–(F5), Özmen (2002) presented the damage percentages based on the 1999 Izmit Earthquake, which was close to Istanbul (Table B2 in Appendix B). The total number of affected people can then be calculated by multiplying the total percentage of the damage states (except "No damage") by the population information.

Herein, as demand items, we consider delivering water purification tablets, medicines, and disposable masks because these are urgent and their low weights and volumes make them easy to transport using small drones. We assume that the weight of the demand items is 0.5 gram for each affected individual. Each demand scenario represents the weight of the packages sent to gathering points and differs based on different earthquake scenarios in terms of the location, depth, and magnitude of the earthquake. Table B3 in Appendix B shows sample demand values for different scenarios. For determining the road distance, we calculate the damage percentages of the depot and launch points and consider their average. We subsequently increase the road distance by the average. Therefore, each road distance scenario corresponds to the percentage increase in the distance between the depots and launch points. Similar to the demand scenarios, they are determined by different earthquake scenarios. Table B4 in Appendix B shows sample road distance percentages for different scenarios. The number of scenarios $|S|$ that we consider for the demand and road network uncertainties is 50. We analyzed ten different scenario sets in terms of earthquake location and magnitude.

The average truck speed $\bar{v}$ is set to 45 kilometers per hour based on the regulations set by the General Directory of Highways of Turkey (Dukkanci et al., 2021). To ensure that all deliveries are completed within a reasonable time, the time-bound T was set as 1 hour. In the computational experiments, we assume that deliveries by small drones directly from depots are omitted. The maximum speed limit for small drones v_{lk} traveling between launch point $l \in L$ and gathering point $k \in K$ is calculated using the range function given in Eq. (1). The maximum speed limit of the large drones $v_{\max}^{BD}$ is set as 30 meters per second (108 kilometers per hour) (Volocopter, 2021). We neglect the impact of the payload weight on the flight range of the large drones because we assume that the large drones are not range limited. The setup time τ of a drone for delivery is set to 2 minutes (Murray & Chu, 2015). The capacities of the small drone Q_{SD} and large drones Q_{BD} are set to 2 kilograms (Techmonitor, 2019) and 200 kilograms (Volocopter, 2021), respectively, whereas the capacity of the trucks Q_T is set to 2000 kilograms. The descriptions and typical values of these parameters are also given in Table B5 of Appendix B. The other parameters are listed in Table A1 of Appendix A.

5.3. Computational analysis using the small dataset

This section presents detailed analyses of the solution to the problem using the small dataset. First, the performance of the SDA is evaluated in comparison with the DEP. Second, we analyze the value of stochasticity and the expected value of perfect information. Finally, we evaluate the impact of equity.

5.3.1. Performance of the scenario decomposition algorithm

In this section, we evaluate the performance of the SDA. We conduct experiments, in which we set the number of depots p to one and two; the number of launch points e is set as four; the number of large drones m^{BD} is set as zero, one, and two; and the number of small drones per launch point $|U|$ is set as two. Because we consider ten different scenario sets, the experiments are conducted over 60 different instances in total. Table 2 compares the results obtained by solving the DEP developed in Section 3.1 and the SDA proposed in Section 4 without and with improvement strategies. In the table, "Obj. Func." and "Sol. Time" represent the objective function value (total unsatisfied demand) in kilograms and solution time in seconds, respectively. Additionally, for the DEP, "Gap" indicates the optimality gap if the optimal solution cannot be found within the two-hour time limit.

The results listed in Table 2 reveal that only three out of 60 instances can be solved by the DEP within the set time limit. For the remaining instances, the average (maximum) optimality gap is 2.58% (20.70%). However, the SDA can solve each of 60 instances to optimality. The average solution time for the DEP and SDA without and with improvement strategies are 6881.86, 245.76 and 224.57 seconds, respectively. The geometric mean of solution time for the respective solution approaches are 6395.76, 233.82 and 214.09 seconds. Therefore, we can conclude that SDA outperforms DEP in terms of solution time and improvement strategies on SDA provide an 8.62% reduction in solution times, on average.

5.3.2. Value of stochasticity and expected value of perfect information

This section presents the analyses of the value of stochasticity (VS) and the expected value of perfect information (EVPI). VS can be considered to be the gain obtained if the problem is solved using stochastic optimization instead of deterministic optimization. In particular, VS is the difference between the solutions obtained by solving the stochastic and deterministic versions of the problem. The stochastic version is solved by the SDA, and the objective function value of the stochastic version (z_S) is determined. To solve the deterministic version, first-stage variables are fixed based on the solution obtained by solving a deterministic problem, in which the expected values of demand and road distance are used. Subsequently, the problem is solved for each scenario using fixed first-stage variables, and the expected objective function value is set as that of the deterministic version (z_D). VS can be calculated as $\frac{z_D - z_S}{z_S}$. Additionally, EVPI is the difference between the solutions obtained by solving the stochastic version of the problem and the other version, in which the exact values of demand and road distance are known in advance. To calculate the objective function value of the other version, each scenario is solved with the exact demand and road distance values, and the expected objective function value (z_P) for all scenarios is thus obtained. The EVPI can be calculated as $\frac{z_P - z_S}{z_S}$.

The experiments are conducted over ten different scenario sets with 180 instances in total, in which the number of depots p is set as one and two; the number of launch points e is set as four, five, and six; the number of large drones m^{BD} is set as zero, one, and two, and the number of small drones $|U|$ per launch point is set as two. Table 3 shows the average values of the results obtained by solving the stochastic version ("SDA"), deterministic version ("Fixed"), and version with the perfect information ("Perfect information") for ten different scenario sets. Additionally, VS and EVPI are reported in the table for the percentages and number of affected people. The number of affected people is roughly estimated by dividing the total unsatisfied demand (the objective function value) by the unit demand weight (0.5 g).

The stochastic and deterministic versions of the problem yield different solutions for 156 out of 180 instances and result in an 8.99% VS on average, which indicates that stochastic optimization covers 784 (3495) more people on average (maximum). The results listed in Table 3 suggest that a large number of depots, small number of launch points, and more large drones increase the value of the stochastic optimization on average in terms of percentages. The perfect information on demand and road network results in different solutions for 111 out of 180 instances. As shown in Table 3, the average EVPI is 1.75%, which indicates that an extra 158 (752) affected people on average (maximum) can be covered using the perfect information. Additionally, the results listed in Table 3 show that a large number of depots, small number of launch points, and more large drones increase the value of the perfect information on average in terms of percentages. Interestingly, Table 3 shows that the expected value of perfect information is zero when using six launch points, which indicates that the same depots and launch points are open for each scenario. As there are only seven candidate launch points, the number of possible combinations (six out of seven) of open launch points is limited; therefore the same network can be expected to be present for different scenarios.

5.3.3. Impact of equity

This section analyses the impact of being equal (fair) on the people at the gathering points by ensuring a visit to each gathering point. To ensure that each gathering point is visited using at least one (large or small) drone, we add the following constraint to the formulation:

$$\sum_{i \in L} \sum_{l \in U} z_{ikls} + \sum_{j \in D} r_{jks} \geq 1 \quad \forall k \in C, s \in S. \tag{23}$$

Table 4 presents the average results over ten different 50-scenario sets with 80 instances in total, in which one and two depots, six and seven launch points, three and four large drones, and two small drones per launch points are considered. We increased the number of launch points and large drones in this experiment to ensure that we obtain feasible solutions to the equity case. In the table, "Obj. Func." and "Gath. Point" represent the objective function value (total unsatisfied demand) and number of gathering points visited (out of 40), respectively, for both cases: the original problem and the problem, in which each gathering point is visited. The final column "Difference" indicates the difference between the two problems in terms of the number of people.

The results reveal that the original problem yields solutions, in which almost all gathering points are visited as the average number is greater than 39.7 for each parameter setting. As this could be related to a large number of launch points and large drones, we can only compare these instances according to the feasibility issue of the new problem. As expected, the number of gathering points according to the new problem is equal to the total number of gathering points (40); however, considering that equity causes an increase in the total unsatisfied demand, which leads to 2000 fewer people being reached on average. Another observation from these experiments is that the impact of considering equity on the total unsatisfied demand is less for a large number of depots, launch points, and large drones. Overall, we can conclude that considering equity has a marginal impact on equity and a negative impact on efficiency.

Here, we remark that the results present only one possible way to analyze the equity issue since we consider equity as visiting each gathering point. Since equity is a quite significant issue in hu-

Table 2
Performance of the scenario decomposition algorithm .

					DEP			SDA		SDA with improvement	
$\|I\|$	p	e	m^{BD}	$\|U\|$	Obj. Func. (kilograms)	Sol. Time (seconds)	Gap (%)	Obj. Func. (kilograms)	Sol. Time (seconds)	Obj. Func. (kilograms)	Sol. Time (seconds)
1	1	4	0	2	9.64	7201.68	0.21	9.64	222.43	9.64	140.75
1	1	4	1	2	7.78	7200.86	0.30	7.78	313.57	7.78	244.48
1	1	4	2	2	6.11	1376.31		6.11	204.65	6.11	188.07
1	2	4	0	2	8.95	348.88		8.95	230.04	8.95	224.38
1	2	4	1	2	6.95	622.74		6.95	276.92	6.95	153.02
1	2	4	2	2	5.44	7200.74	0.03	5.44	286.24	5.44	218.04
2	1	4	0	2	6.16	7201.29	0.81	6.15	137.85	6.15	141.50
2	1	4	1	2	4.61	7203.81	0.83	4.61	249.23	4.61	234.04
2	1	4	2	2	3.33	7201.44	0.95	3.33	177.48	3.33	150.61
2	2	4	0	2	5.77	7203.27	2.80	5.77	245.55	5.77	234.78
2	2	4	1	2	4.25	7202.36	3.94	4.25	333.80	4.25	346.64
2	2	4	2	2	2.98	7203.09	5.01	2.98	234.24	2.98	251.27
3	1	4	0	2	7.17	7200.95	0.24	7.17	122.76	7.17	117.91
3	1	4	1	2	5.52	7202.66	0.30	5.52	266.20	5.52	202.30
3	1	4	2	2	4.07	7201.72	0.46	4.07	168.89	4.07	148.56
3	2	4	0	2	6.68	7202.81	0.19	6.68	172.90	6.68	163.13
3	2	4	1	2	4.98	7202.02	0.73	4.98	261.79	4.98	293.94
3	2	4	2	2	3.64	7201.00	0.70	3.64	204.71	3.64	168.12
4	1	4	0	2	8.93	7204.76	0.57	8.92	153.71	8.92	211.66
4	1	4	1	2	7.02	7201.83	0.56	7.02	449.40	7.02	265.39
4	1	4	2	2	5.50	7201.77	0.63	5.50	198.37	5.50	211.92
4	2	4	0	2	8.25	7201.26	0.24	8.25	256.84	8.25	202.37
4	2	4	1	2	6.34	7200.84	0.25	6.34	307.15	6.34	298.00
4	2	4	2	2	4.87	7202.24	0.22	4.87	296.36	4.87	291.53
5	1	4	0	2	8.94	7205.93	0.34	8.94	202.80	8.94	189.86
5	1	4	1	2	6.93	7202.33	0.38	6.93	373.90	6.93	307.42
5	1	4	2	2	5.44	7202.06	0.38	5.44	511.40	5.44	219.67
5	2	4	0	2	8.07	7217.30	0.40	8.07	178.89	8.07	163.48
5	2	4	1	2	6.07	7201.54	0.18	6.07	214.96	6.07	171.20
5	2	4	2	2	4.66	7201.84	0.25	4.66	246.36	4.66	223.37
6	1	4	0	2	4.84	7201.52	0.76	4.84	215.71	4.84	169.15
6	1	4	1	2	3.49	7202.51	1.02	3.49	310.02	3.49	425.25
6	1	4	2	2	2.34	7203.72	1.53	2.34	293.52	2.34	322.30
6	2	4	0	2	4.52	7201.64	7.29	4.35	401.03	4.35	329.76
6	2	4	1	2	3.25	7202.57	10.14	3.07	361.61	3.07	405.57
6	2	4	2	2	2.16	7201.82	16.11	1.96	264.82	1.96	289.70
7	1	4	0	2	9.00	7205.86	0.65	9.00	188.67	9.00	223.13
7	1	4	1	2	7.00	7201.83	0.67	7.00	338.57	7.00	298.75
7	1	4	2	2	5.33	7201.93	0.75	5.33	245.67	5.33	239.48
7	2	4	0	2	8.02	7222.70	0.70	8.02	302.89	8.02	347.76
7	2	4	1	2	6.12	7202.55	0.48	6.12	348.94	6.12	249.02
7	2	4	2	2	4.66	7202.61	0.63	4.66	334.98	4.66	344.96
8	1	4	0	2	4.41	7203.02	1.48	4.39	172.48	4.39	148.27
8	1	4	1	2	3.17	7203.09	1.75	3.17	275.56	3.17	235.57
8	1	4	2	2	2.09	7203.01	3.17	2.09	212.16	2.09	167.38
8	2	4	0	2	4.17	7201.47	9.61	3.93	177.84	3.93	179.21
8	2	4	1	2	3.01	7202.17	13.00	2.78	288.58	2.78	374.04
8	2	4	2	2	1.98	7201.96	20.70	1.72	218.90	1.72	223.94
9	1	4	0	2	7.14	7200.83	0.49	7.14	123.30	7.14	121.83
9	1	4	1	2	5.37	7202.17	0.62	5.37	236.99	5.37	211.99
9	1	4	2	2	3.95	7203.09	0.80	3.95	247.39	3.95	162.45
9	2	4	0	2	6.59	7200.69	0.47	6.59	181.39	6.59	177.40
9	2	4	1	2	4.85	7202.78	0.88	4.85	281.81	4.85	244.94
9	2	4	2	2	3.49	7202.46	2.32	3.49	192.37	3.49	201.13
10	1	4	0	2	4.96	7203.10	0.23	4.96	137.21	4.96	149.25
10	1	4	1	2	3.50	7203.12	0.31	3.50	205.65	3.50	204.24
10	1	4	2	2	2.33	7201.27	0.27	2.33	201.26	2.33	148.06
10	2	4	0	2	4.67	7201.68	5.23	4.58	136.16	4.58	182.24
10	2	4	1	2	3.27	7201.25	8.61	3.13	224.01	3.13	170.13
10	2	4	2	2	2.11	7202.13	14.35	1.95	126.90	1.95	149.91
		Average				6881.86	2.58		245.76		224.57
		Geometric mean				6395.76			233.82		214.09

manitarian applications to ensure a fair distribution of relief items to affected people, the humanitarian logistics literature captures equity by considering different constraints and objective functions. For instance, equity can be covered by ensuring a certain part of the demand is satisfied for each gathering point similar to the equitable supply allocation policies in the studies of Noyan et al. (2016); Noyan & Kahvecioğlu (2018). Other examples to incorporate equity into relief logistics problems are modeling objective functions (i) to minimize the maximum unsatisfied demand (or maximize the minimum demand coverage as in the studies of Battarra et al., 2018; Tzeng et al., 2007), (ii) to minimize the total or maximum difference of unsatisfied demand among all gathering points as in the study of Mohammadi et al. (2016) or (iii) to minimize a piecewise-linear disutility function based on the unsatisfied de-

Table 3
Value of stochasticity and expected value of perfect information.

				SDA	Fixed			Perfect information		
p	e	m^{BD}	|U|	Obj. Func. (kilograms)	Obj. Func. (kilograms)	VS (%)	VS (# people)	Obj. Func. (kilograms)	EVPI (%)	EVPI (# people)
1	4	0	2	7.11	7.76	8.52	1291	7.05	1.07	137
1	4	1	2	5.44	6.07	10.87	1259	5.37	1.48	143
1	4	2	2	4.05	4.65	14.05	1213	3.96	2.62	182
1	5	0	2	5.83	6.06	3.96	457	5.76	1.08	138
1	5	1	2	4.17	4.31	3.34	289	4.10	1.46	135
1	5	2	2	2.81	3.02	7.10	417	2.75	1.69	115
1	6	0	2	5.48	5.63	2.43	291	5.48	0.00	0
1	6	1	2	3.82	3.97	3.72	300	3.82	0.00	0
1	6	2	2	2.49	2.64	4.12	295	2.49	0.00	0
2	4	0	2	6.52	6.90	5.50	759	6.23	4.53	579
2	4	1	2	4.85	5.47	11.26	1231	4.57	5.90	559
2	4	2	2	3.54	3.91	9.06	745	3.27	7.83	533
2	5	0	2	5.32	5.87	9.59	1085	5.26	0.97	119
2	5	1	2	3.69	4.03	10.05	692	3.64	1.14	103
2	5	2	2	2.40	2.89	18.44	974	2.35	1.67	102
2	6	0	2	5.02	5.39	6.48	753	5.02	0.00	0
2	6	1	2	3.40	3.80	10.53	792	3.40	0.00	0
2	6	2	2	2.13	2.76	22.77	1274	2.13	0.00	0
Average				4.34	5.10	8.99	784	4.26	1.75	158

Table 4
Impact of equity.

				No equity		Equity		
p	e	m^{BD}	|U|	Obj. Func. (kilograms)	Gath. Point	Obj. Func. (kilograms)	Gath. Point	Difference
1	6	3	2	1.31	39.73	2.76	40.00	2904
1	6	4	2	1.02	39.77	2.09	40.00	2124
1	7	3	2	1.22	39.72	2.33	40.00	2221
1	7	4	2	0.93	39.76	1.67	40.00	1488
2	6	3	2	1.01	39.76	2.25	40.00	2476
2	6	4	2	0.76	39.76	1.62	40.00	1737
2	7	3	2	0.92	39.77	1.88	40.00	1916
2	7	4	2	0.67	39.81	1.27	40.00	1206
Average				0.98	39.76	1.98	40.00	2009

mand over time ensuring that first deliveries to a gathering point are more important than the latter ones to promote equity as in the study of Huang et al. (2012). Recently, research also studies the deprivation cost introduced by Holguín-Veras et al. (2013), which is defined to economically quantify human suffering due to lack of access to relief items. Several studies use deprivation cost to provide equitable allocation over time (Moreno et al., 2018; Pérez-Rodríguez & Holguín-Veras, 2016).

5.3.4. Analysis on the number of drones

This section presents an analysis of another important strategic extension of our problem, in which the aim is to find solutions with the minimum number of (small and large) drones given a certain percentage of the demand is satisfied. Finding the ideal number of transportation resources is quite significant to have a more efficient system before a possible earthquake without spending too much money on the fleet. In particular, having drones as part of the required fleet makes this extension more relevant for practitioners as drones are relatively new technology and might not be already available.

An ideal way to solve this extension is to revise the mathematical formulation given in Section 3.1. In particular, the objective function should be updated to minimize the number of vehicles and a constraint should be included to make sure that a certain percentage of demand is satisfied. Alternatively, here, we implement an algorithmic search, in which we change the number of (small and large) drones to find solutions for this extension. Table 5 shows the number of drones used for ten different 50-scenario sets given a 90% demand coverage. The first three columns of Table 5 indicate the number of depots (p), the number of launch points (e) and the number of small drones per launch point (|U|), respectively. While the fourth columns represent the number of small drones (m^{SD}), the remaining columns (except the last two) show the number of large drones (m^{BD}) used for ten different sets. Finally, the last two columns indicate the average number of large drones and the average number of all (small and large) drones, respectively.

Table 5
Ideal number of drones.

p	e	|U|	m^{SD}	m^{BD}										m^{SD} & m^{BD}
				1	2	3	4	5	6	7	8	9	10	Average	Total
1	5	1	5	10	7	8	9	9	6	9	6	8	6	7.8	12.8
1	5	2	10	3	1	2	2	3	1	2	1	1	1	1.7	11.7
1	6	1	6	9	6	6	7	8	5	8	5	6	5	6.5	12.5
1	6	2	12	3	1	2	2	2	1	2	0	1	1	1.5	13.5
1	7	1	7	8	5	6	6	7	4	7	4	5	5	5.7	12.7
1	7	2	14	3	1	1	2	2	1	2	0	1	1	1.4	15.4
2	5	1	5	9	6	7	8	9	5	8	5	7	5	6.9	11.9
2	5	2	10	3	1	1	2	2	1	2	0	1	1	1.4	11.4
2	6	1	6	8	5	5	6	7	4	7	3	5	4	5.4	11.4
2	6	2	12	3	1	1	2	2	0	1	0	1	1	1.2	13.2
2	7	1	7	7	4	5	6	6	3	6	3	4	3	4.7	11.7
2	7	2	14	2	1	1	1	2	0	1	0	1	1	1.0	15.0

Here, we first remark that due to the consideration of different scenarios over these ten different scenario sets, the change in

the number of big drones can be easily observed to satisfy the 90% demand coverage. Additionally, further analysis of the solutions shows that increasing the number of depots (from 1 to 2) has a marginal impact on the number of drones used (3.66% for large drones and 1.15% for all drones). On the other hand, having six or seven launch points instead of five reduces the number of large drones by 17.98% and 28.09%, respectively, and it increases the number of all drones by 5.86% and 14.64% due to the increase in the number of small drones. Finally, we observe that having two small drones per launch point instead of one reduces the number of large drones used by 77.84%, but increases the number of all drones by 9.86%.

5.4. Computational analysis using the large dataset

Herein, we present the results of the computational analysis using the large dataset. First, a clustering approach is proposed to solve this dataset. Second, the computational results are discussed for different settings by changing the number of depots p, number of launch points e, number of large drones m^{BD}, number of small drones $|U|$ per launch point, time-bound T, and capacity of the small drones Q_{SD}.

5.4.1. Clustering approach

Although the SDA outperforms DEP in terms of solution time over instances generated by the small dataset (Section 5.3.1), SDA could not solve the large dataset mentioned in Section 5.1 within a reasonable time. Therefore, we present a heuristic approach based on the clustering of gathering points to reduce the size of the problem, such that SDA can solve the problem.

Before clustering, we apply a preprocessing approach to eliminate the gathering points that are inaccessible under the predetermined time bound. The main aim of this preprocessing approach is to exclude these inaccessible gathering points, which are unlikely to be clustered with the other points, and to improve the clustering of the remaining accessible gathering points. If the travel time between a gathering point and launch point and the minimum travel time between the launch point and (the closest) depot is greater than the predetermined time bound (T) for each possible launch point, then that gathering point is inaccessible from any launch point and removed from the list of gathering points for clustering. Before clustering, we also assign large drones (if any) to the gathering points. Because they perform only one delivery in the proposed problem, they cannot be sent to a cluster to distribute relief items. To effectively use the high capacities of large drones, they are assigned to serve the gathering points with the highest demands.

After the preprocessing approach and assignment of the large drones, the remaining gathering points are clustered using the k-means algorithm. To solve this problem after clustering, we define some new parameters (Table B6 of Appendix B). As the distance and drone speed between a launch point and a gathering point are fixed, we can calculate the travel time between a launch point and a gathering point (t_{lk}). Therefore, we can calculate the travel time between a launch point and a cluster (ψ_{lg}), which is the summation of travel times between the launch point and all gathering points in the same cluster ($\sum_{h\in C_g} t_{lh}$). The main aim of defining these time-related parameters is to ensure that the time bound constraint is satisfied for clustered gathering points. Similarly, if the demand at the gathering points for each scenario (ξ_{ks}) is known, we can calculate the total demand of a cluster for a scenario (σ_{gs}), which is the summation of the demand at all the gathering points in the same cluster ($\sum_{h\in C_g} \xi_{hs}$). This parameter is defined to adhere to the truck capacity constraint. Here, we define another parameter related to the demand for the objective function. Although the parameter σ_{gs} can be used in the objective function, using the demand of a cluster may lead to an increase in the total unsatisfied demand over all the gathering points in the clustering approach. For instance, let us assume that a cluster is formed with three gathering points, all of which have 1.5 kilograms of demand (in total 4.5 kilograms), and the capacity of a small drone is 2 kilograms. If σ_{gs} is used in the objective function, three drones can be sent to that cluster to satisfy all demands according to the optimal solution. However, in reality, only one drone is sufficient because this drone can satisfy the demand for each gathering point in that cluster. Therefore, we define a new demand parameter that represents the maximum demand of a cluster for a scenario (χ_{gs}), which is the maximum demand of all gathering points in the same cluster ($\max_{\{h\in C_g\}} \xi_{hs}$). While calculating the unsatisfied demand, the parameter χ_{gs} is used.

The formulation solved within the SDA after clustering is given as

$$\text{Minimize} \quad \sum_{s\in S} p_s \sum_{g\in G} o_{gs} \tag{24}$$

subject to

(3)–(6), (13)–(15)

$$\sum_{u\in U}\sum_{g\in G} \sigma_{gs} z_{lgus} \le Q_T y_l \qquad \forall l \in L, s \in S \tag{25}$$

$$\chi_{gs}\phi_g - Q_{SD}\phi_g \sum_{l\in L}\sum_{u\in U} z_{lgus} \le o_{gs} \qquad \forall g \in G, s \in S \tag{26}$$

$$\sum_{j\in D} \frac{\omega_{ljs}}{\bar{v}} w_{lj} + \sum_{g\in G} (2\psi_{lg} + \tau\phi_g) z_{lgus} \le T \qquad \forall l \in L, u \in U, s \in S \tag{27}$$

$$z_{lgus} \in \{0,1\} \qquad \forall l \in L, g \in G, u \in U, s \in S \tag{28}$$

$$o_{gs} \ge 0 \qquad \forall g \in G, s \in S. \tag{29}$$

Objective function (24) minimizes the unsatisfied demand for all clusters. Constraint (25) is the truck capacity constraint. Constraint (26) calculates the unsatisfied demand for each cluster and scenario. The left-hand side of this constraint is multiplied by the number of customers in a cluster to improve the representation of the clusters. Constraint (27) is the new time bound constraints for the small drones. While the first term on the left-hand side represents the (uncertain) truck travel time between depots and launch points, the second term represents the total drone travel time between launch points and clusters. Constraints (28) and (29) define the variable domains.

When the above formulation is solved within the SDA, we know which clusters are visited in each scenario. Thus, we know which gathering points are visited in each scenario. Therefore, we can easily calculate the total unsatisfied demand over all gathering points. Algorithm 1 in Appendix B presents the steps of the clustering approach.

5.4.2. Performance of the clustering approach

We first analyze the performance of the clustering approach over the small dataset by using the same parametric settings that we used in Section 5.3.1. Table 6 shows the average results obtained by the SDA and the clustering approach over ten different 50-scenario sets. We cluster 40 gathering points in the small dataset into 20 clusters. Unlike in Table 2, "Gap" represents the difference of the objective functions divided by the total demand to obtain the reduced percentage of the satisfied demand.

The results in Table 6 show that the average gap was approximately 5%, which indicates that the clustering approach yields a solution with a 5% reduction in the satisfied demand on average. Additionally, the clustering approach was able to find the solution within a few seconds.

Table 6
Performance of the clustering approach.

				SDA		Clustering approach		
p	e	m^{BD}	|U|	Obj. Func. (kilograms)	Sol. Time (seconds)	Obj. Func. (kilograms)	Sol. Time (seconds)	Gap (%)
1	4	0	2	7.11	160.65	7.74	2.55	1.63
1	4	1	2	5.44	262.19	7.29	2.48	4.90
1	4	2	2	4.05	195.33	6.71	6.29	7.10
2	4	0	2	6.52	219.61	7.51	3.92	2.62
2	4	1	2	4.85	269.56	7.06	3.78	5.85
2	4	2	2	3.54	235.34	6.71	10.40	8.45
Average				5.25	223.78	7.17	4.91	5.09

Table 7
Average results using the large dataset.

			Two small drones		Three small drones	
p	e	m^{BD}	Uns. Demand (kilograms)	People	Uns. Demand (kilograms)	People
1	2	0	317.55	635,101	303.26	606,526
1	2	1	314.83	629,657	300.64	601,275
1	2	2	313.41	626,822	299.47	598,938
1	3	0	303.92	607,843	285.42	570,849
1	3	1	301.19	602,384	282.78	565,556
1	3	2	299.77	599,538	281.65	563,303
1	4	0	290.50	580,993	268.54	537,076
1	4	1	287.75	575,493	265.91	531,813
1	4	2	286.37	572,746	264.79	529,572
1	5	0	279.62	559,231	248.62	497,235
1	5	1	276.90	553,795	245.88	491,767
1	5	2	275.47	550,939	244.69	489,375
1	6	0	267.23	534,465	237.55	475,105
1	6	1	264.45	528,891	234.80	469,601
1	6	2	263.02	526,036	233.64	467,283
2	2	0	313.78	627,566	298.84	597,673
2	2	1	311.14	622,282	296.27	592,531
2	2	2	309.78	619,564	295.08	590,162
2	3	0	295.51	591,014	278.48	556,969
2	3	1	292.86	585,722	275.94	551,881
2	3	2	291.47	582,940	274.76	549,524
2	4	0	284.53	569,051	260.98	521,967
2	4	1	281.84	563,679	258.41	516,821
2	4	2	280.41	560,812	257.28	514,557
2	5	0	270.48	540,958	242.82	485,649
2	5	1	267.76	535,527	240.18	480,368
2	5	2	266.36	532,714	239.10	478,210
2	6	0	257.09	514,175	225.92	451,833
2	6	1	254.36	508,715	223.27	446,546
2	6	2	252.90	505,798	222.21	444,421

5.4.3. Computational analysis

This section presents the sensitivity analyses for certain parameters of the problem, including the number of depots (p), number of launch points (e), number of large drones (m^{BD}), number of small drones ($|U|$) per launch point, time-bound (T), and capacity of the small drones (Q_{SD}). Similar to the analysis conducted using the small dataset (Section 5.3), we consider ten different scenario sets consisting of 50 scenarios each. For these analyses, we apply the clustering approach to the large dataset, in which 365 gathering points are clustered to form 100 clusters.

Table 7 lists the average results for ten different scenario sets with the number of depots p is set as one and two; number of launch points e is set as two, three, four, five, and six; number of large drones m^{BD} is set as zero, one, and two; and number of small drones $|U|$ per launch point is set as two and three. Columns "Uns. Demand" and "People" represent the total unsatisfied demand in kilograms and the approximate number of people who did not receive relief items within 1 hour, respectively.

The results shown in Table 7 indicate the following observations: (i) increasing the number of small drones per launch point from two to three reduces the total unsatisfied demand by 7.99%, on average; (ii) increasing the number of depots to be opened from one to two reduces the total unsatisfied demand by 2.64%; (iii) Fig. 4 shows the reduction in the total unsatisfied demand in percentages when the number of launch points to be used is increased from two to three, four, five, and six; and (iv) finally, having one and two large drones decreases the total unsatisfied demand by 0.97% and 1.43%, respectively, with respect to the case without large drones.

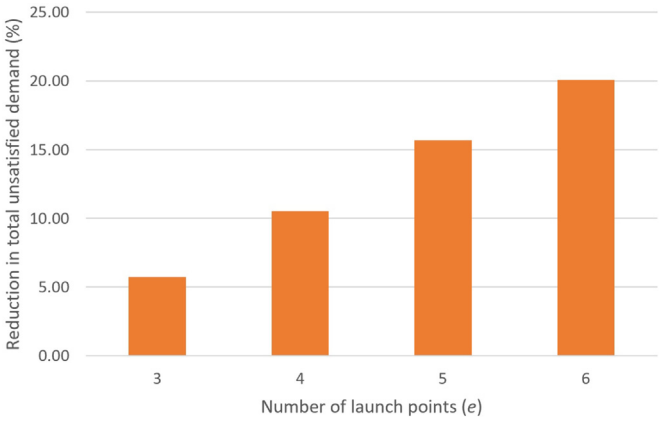

Fig. 4. Percentage reduction in the total unsatisfied demand with different number of launch points.

Overall, the results suggest that increasing the number of launch points or the number of small drones per launch point has a larger impact on the total unsatisfied demand than increasing the number of depots or number of large drones because having more depots only affects the assignment of launch points to depots and having more large drones affects one or two gathering points only. Having more launch points or small drones per launch point increases the total number of small drones and, therefore, the total satisfied demand.

Furthermore, we analyzed the impact of considering different time bounds to complete all deliveries. More details of the experiments can be found in Table B7 of Appendix B. The last three rows of the table indicate the average, minimum, and maximum results over 12 different settings, which are also depicted in Fig. 5(a) in terms of the percentage change in total unsatisfied demand.

The results listed in Table B7 of Appendix B show that increasing the time bound from 60 minutes to 90 and 120 minutes reduces the total unsatisfied demand by 7.88% and 14.98%, respectively, on average. In contrast, using a tight time bound of 30 minutes causes an average 9.28% increase in the total unsatisfied demand. Additionally, the results suggest that having more depots reduces the percentage changes for loose time bounds and increases these changes for tight time bounds, which indicates that a small number of depots is preferred. A large number of launch points increases the percentage changes for loose and tight time bounds, thereby suggesting that for tight and loose time bounds, a small and large number of launch points, respectively, are preferable. The number of large drones does not result in a particular trend. The 30-min time bound yields the lowest percentage change when one depot, two launch points, and two large drones are used. Additionally, for loose time bounds, two depots and two launch points without any large drones yield the lowest percentage change. The highest percentage change is observed for the tight time-bound when the two depots and three launch points are used, and for loose time bounds, one depot and three launch points are used with two large drones.

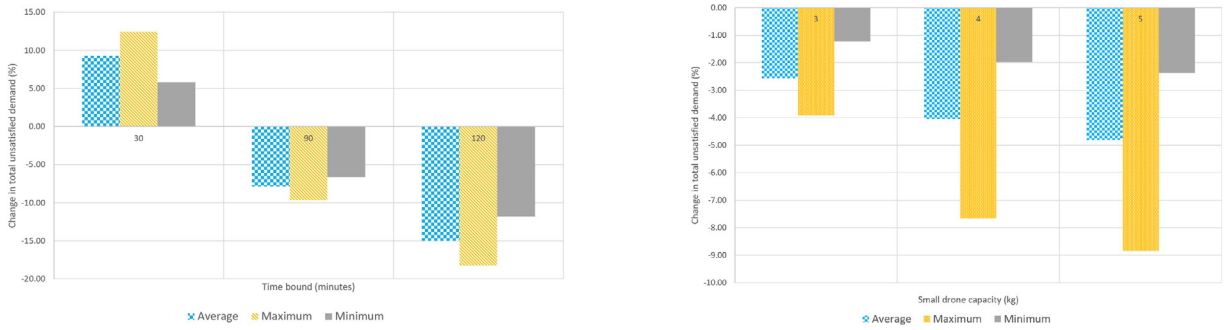

(a) Different time bounds (b) Different capacities for small drones

Fig. 5. Percentage reduction in the total unsatisfied demand.

Herein, we present a sensitivity analysis of the capacity of the small drones. More details of the experiments can be found in Table B8 of Appendix B. Fig. 5(b) shows the average, minimum, and maximum changes over 24 different parametric settings, which are also listed in the last three rows of the table.

The results listed in Table B8 of Appendix B indicate that increasing the capacity of the small drones to 3, 4, and 5 kilograms reduces the total unsatisfied demand by 2.56%, 4.04% and 4.81% on average, respectively. This suggests that the greatest reduction achieved owing to a 1 kilogram increase occurred when the capacity is extended to 3 kilograms. For all capacity values considered in this analysis, the smallest percentage changes are observed when the time bound is set as 1 hour and one depot and two launch points are used with two large drones. The highest percentage changes are observed for all capacity values when the time bound is set as 2 hours and 3 launch points are used. However, when the capacity is 3 kilograms, using two depots yields the highest percentage change, and when the capacity is increased to 4 or 5 kilograms, using only one depot yields the highest percentage change.

6. Conclusions

This study introduces the relief distribution problem using drones under uncertainty, in which relief items are delivered to affected people using small and/or large drones in an uncertain environment in terms of demand at gathering points and road network. The main aim of the problem is to minimize the total unsatisfied demand at all the gathering points while ensuring that the deliveries are completed within the given time bound. Additionally, the range of the small drones, as well as the capacities of the small and large drones and trucks, should not be exceeded during deliveries. The problem is first modeled as a two-stage stochastic program, and then its deterministic equivalent problem is presented. An SDA is developed to solve real-life-sized instances. A case study based on a post-disaster application in Istanbul, Turkey, was conducted because an earthquake is expected to occur in that area. To consider the demand and road network uncertainties, different earthquake scenarios in terms of location and magnitude are generated. Computational experiments are conducted over small and large datasets to evaluate the performance of the SDA, analyze the stochastic optimization and perfect information, and examine the results under different parametric settings.

Extensive computational analyses allowed the derivation of the following practical implications: (i) considering uncertainties of demand and road network increases the number of people who can receive relief items over a short duration, (ii) practitioners should focus on increasing the numbers of launch points and small drones instead of the numbers of depots and large drones as the former two have a high impact on reducing the unsatisfied demand, (iii) if practitioners consider loose time bounds and use drones with a large capacity, they should increase the number of launch points as much as possible but not the number of depots. The theoretical implications are as follows: for the first time, our results presented solutions of a two-echelon distribution problem with range-limited drones and trucks under demand and road network uncertainties while aiming to minimize the total unsatisfied demand. Our results also revealed that the SDA is a powerful solution approach compared to the DEP formulation when applying a small dataset, and a heuristic approach must be employed to solve a large dataset of this stochastic problem. Even the deterministic version applying the large dataset cannot be solved.

Our research and findings are limited to certain situations because of the following assumptions: (i) weather conditions that may affect the operations of drones are neglected, (ii) the number of fully-charged batteries in trucks are sufficient to ensure that small drones can operate without recharging, (iii) large drones are not range limited and the payload weight has no impact on their flight ranges. Additionally, our computational results over the large instance are limited by the heuristic solutions.

In future research, different objective functions can be a promising area to investigate further. Although this problem is considered from a humanitarian perspective by minimizing the total unsatisfied demand, the economic impacts of such a problem can be considered, for instance, by minimizing the total cost, including the fixed cost of locating depots, transportation costs of the trucks and drones and the penalty cost of the unsatisfied demand. Another potential objective function can be minimizing the number of vehicles (drones) while ensuring a certain demand satisfaction. Another interesting future research area can be to consider other possible uncertainties of the proposed relief distribution network, for instance, the uncertainty of drone operations, in particular, the impact of unpredictable weather conditions on drones. Finally, more solution approaches could be studied in the future, especially, to solve the large datasets, different metaheuristics, such as tabu search or genetic algorithms can be implemented.

Acknowledgments

The authors thank the anonymous reviewers and editor for their valuable comments on an earlier version of this paper that resulted in improved content and exposition.

Supplementary material

Supplementary material associated with this article can be found, in the online version, at doi:10.1016/j.ejor.2023.02.038.

References

Ahmed, S. (2013). A scenario decomposition algorithm for 0–1 stochastic programs. *Operations Research Letters, 41*(6), 565–569.

Amazon (2022). Amazon Prime Air prepares for drone deliveries. Available from: https://www.aboutamazon.com/news/transportation/amazon-prime-air-prepares-for-drone-deliveries [Accessed 5 September 2022].

Anaya-Arenas, A. M., Renaud, J., & Ruiz, A. (2014). Relief distribution networks: A systematic review. *Annals of Operations Research, 223*(1), 53–79.

Balfour Beatty (2017). Flying into the future of bridge inspections. May 12, 2017. Available from: https://www.balfourbeatty.com/news/flying-into-the-future-of-bridge-inspections/ [Accessed 5 September 2022].

Battarra, M., Balcik, B., & Xu, H. (2018). Disaster preparedness using risk-assessment methods from earthquake engineering. *European Journal of Operational Research, 269*(2), 423–435.

Bayrak, E., Nas, M., & Bayrak, Y. (2019). New macroseismic intensity predictive models for turkey. *Acta Geophysica, 67*(6), 1483–1513.

Chauhan, D., Unnikrishnan, A., & Figliozzi, M. (2019). Maximum coverage capacitated facility location problem with range constrained drones. *Transportation Research Part C: Emerging Technologies, 99*, 1–18.

Chauhan, D. R., Unnikrishnan, A., Figliozzi, M., & Boyles, S. D. (2021). Robust maximum coverage facility location problem with drones considering uncertainties in battery availability and consumption. *Transportation Research Record, 2675*(2), 25–39.

Chowdhury, S., Emelogu, A., Marufuzzaman, M., Nurre, S. G., & Bian, L. (2017). Drones for disaster response and relief operations: A continuous approximation model. *International Journal of Production Economics, 188*, 167–184.

Chung, S. H., Sah, B., & Lee, J. (2020). Optimization for drone and drone-truck combined operations: A review of the state of the art and future directions. *Computers and Operations Research, 123*, 105004.

DHL (2018). Rapid response from the air: Medicines successfully delivered using a parcel drone in east africa. October 4, 2018. Available from: https://www.dhl.com/global-en/home/press/press-archive/2018/rapid-response-from-the-air-medicines-successfully-delivered-using-a-parcel-drone-in-east-africa.html [Accessed 5 September 2022].

Dorling, K., Heinrichs, J., Messier, G. G., & Magierowski, S. (2017). Vehicle routing problems for drone delivery. *IEEE Transactions on Systems, Man, and Cybernetics: Systems, 47*(1), 70–85.

Dukkanci, O., Kara, B. Y., & Bektaş, T. (2021). Minimizing energy and cost in range-limited drone deliveries with speed optimization. *Transportation Research Part C: Emerging Technologies, 125*, 102985.

Erbeyoğlu, G., & Bilge, Ü. (2020). A robust disaster preparedness model for effective and fair disaster response. *European Journal of Operational Research, 280*(2), 479–494.

Erdik, M., & Eren, K. (1983). *Attenuation of intensities for earthquake associated with the north anatolian fault*. Ankara: Middle East Technical University Earthquake Engineering Research Center.

Faiz, T. I., Vogiatzis, C. et al. (2020). Robust two echelon vehicle and drone routing for post disaster humanitarian operations. arXiv preprint arXiv:2001.06456

Fikar, C., Gronalt, M., & Hirsch, P. (2016). A decision support system for coordinated disaster relief distribution. *Expert Systems with Applications, 57*, 104–116.

Gentili, M., Mirchandani, P. B., Agnetis, A., & Ghelichi, Z. (2022). Locating platforms and scheduling a fleet of drones for emergency delivery of perishable items. *Computers & Industrial Engineering, 168*, 108057.

Golabi, M., Shavarani, S. M., & Izbirak, G. (2017). An edge-based stochastic facility location problem in UAV-supported humanitarian relief logistics: A case study of tehran earthquake. *Natural Hazards, 87*(3), 1545–1565.

Grass, E., & Fischer, K. (2016). Two-stage stochastic programming in disaster management: A literature survey. *Surveys in Operations Research and Management Science, 21*(2), 85–100.

Grass, E., Fischer, K., & Rams, A. (2020). An accelerated l-shaped method for solving two-stage stochastic programs in disaster management. *Annals of Operations Research, 284*(2), 557–582.

Holguín-Veras, J., Pérez, N., Jaller, M., Van Wassenhove, L. N., & Aros-Vera, F. (2013). On the appropriate objective function for post-disaster humanitarian logistics models. *Journal of Operations Management, 31*(5), 262–280.

Huang, M., Smilowitz, K., & Balcik, B. (2012). Models for relief routing: Equity, efficiency and efficacy. *Transportation Research Part E: Logistics and Transportation Review, 48*(1), 2–18.

Jeong, H. Y., David, J. Y., Min, B.-C., & Lee, S. (2020). The humanitarian flying warehouse. *Transportation Research Part E: Logistics and Transportation Review, 136*, 101901.

Kim, D., Lee, K., & Moon, I. (2019). Stochastic facility location model for drones considering uncertain flight distance. *Annals of Operations Research, 283*(1), 1283–1302.

Kyriakakis, N. A., Marinaki, M., Matsatsinis, N., & Marinakis, Y. (2022). A cumulative unmanned aerial vehicle routing problem approach for humanitarian coverage path planning. *European Journal of Operational Research, 300*(3), 992–1004.

Lewis, N. (2020). A tech company engineered drones to deliver vital COVID-19 medical supplies to rural ghana and rwanda in minutes. May 12, 2020. Available from: https://www.businessinsider.com/zipline-drone-coronavirus-supplies-africa-rwanda-ghana-2020-5 [Accessed 5 September 2022].

Li, H., Chen, J., Wang, F., & Bai, M. (2021). Ground-vehicle and unmanned-aerial-vehicle routing problems from two-echelon scheme perspective: A review. *European Journal of Operational Research, 294*(3), 1078–1095.

Macias, J. E., Angeloudis, P., & Ochieng, W. (2020). Optimal hub selection for rapid medical deliveries using unmanned aerial vehicles. *Transportation Research Part C: Emerging Technologies, 110*, 56–80.

Macrina, G., Pugliese, L. D. P., Guerriero, F., & Laporte, G. (2020). Drone-aided routing: A literature review. *Transportation Research Part C: Emerging Technologies, 120*, 102762.

Manalo, M. (2015). This budget airline is doing something really smart with drones — and big airlines should pay attention. Business Insider. June 13, 2015. Available from: http://www.businessinsider.com/easyjet-uk-uses-drones-airplane-inspection-2015-6 [Accessed 5 September 2022].

Meola, A. (2021). Precision agriculture in 2021: The future of farming is using drones and sensors for efficient mapping and spraying. Available from: https://www.businessinsider.com/agricultural-drones-precision-mapping-spraying [Accessed 5 September 2022].

Mohammadi, R., Ghomi, S. F., & Jolai, F. (2016). Prepositioning emergency earthquake response supplies: A new multi-objective particle swarm optimization algorithm. *Applied Mathematical Modelling, 40*(9–10), 5183–5199.

Moreno, A., Alem, D., Ferreira, D., & Clark, A. (2018). An effective two-stage stochastic multi-trip location-transportation model with social concerns in relief supply chains. *European Journal of Operational Research, 269*(3), 1050–1071.

Murray, C. C., & Chu, A. G. (2015). The flying sidekick traveling salesman problem: Optimization of drone-assisted parcel delivery. *Transportation Research Part C: Emerging Technologies, 54*, 86–109.

Murray, C. C., & Raj, R. (2020). The multiple flying sidekicks traveling salesman problem: Parcel delivery with multiple drones. *Transportation Research Part C: Emerging Technologies, 110*, 368–398.

Noyan, N., Balcik, B., & Atakan, S. (2016). A stochastic optimization model for designing last mile relief networks. *Transportation Science, 50*(3), 1092–1113.

Noyan, N., & Kahvecioğlu, G. (2018). Stochastic last mile relief network design with resource reallocation. *OR Spectrum, 40*(1), 187–231.

Otto, A., Agatz, N., Campbell, J., Golden, B., & Pesch, E. (2018). Optimization approaches for civil applications of unmanned aerial vehicles UAVs or aerial drones: A survey. *Networks, 72*(4), 411–458.

Özmen, B. (2002). Istanbul ili için deprem senaryosu. *Türkiye Mühendislik Haberleri, 427*, 23–28.

Pérez-Rodríguez, N., & Holguín-Veras, J. (2016). Inventory-allocation distribution models for postdisaster humanitarian logistics with explicit consideration of deprivation costs. *Transportation Science, 50*(4), 1261–1285.

Rabta, B., Wankmüller, C., & Reiner, G. (2018). A drone fleet model for last-mile distribution in disaster relief operations. *International Journal of Disaster Risk Reduction, 28*, 107–112.

ReportLinker (2021). The overall drone inspection and monitoring market is projected to grow from USD 9.1 billion in 2021 to USD 33.6 billion by 2030, at a CAGR of 15.7%. Available from: https://finance.yahoo.com/news/overall-drone-inspection-monitoring-market-082500446.html [Accessed 5 September 2022].

Shavarani, S. M. (2019). Multi-level facility location-allocation problem for post-disaster humanitarian relief distribution. *Journal of Humanitarian Logistics and Supply Chain Management, 9*(1), 70–81.

Stolaroff, J. K., Samaras, C., O'Neill, E. R., Lubers, A., Mitchell, A. S., & Ceperley, D. (2018). Energy use and life cycle greenhouse gas emissions of drones for commercial package delivery. *Nature Communications, 9*(1), 409.

Techmonitor (2019). Amazon's new delivery drone: Five key things we know so far. Available from: https://techmonitor.ai/technology/data/amazon-delivery-drone [Accessed 5 September 2022].

Tofighi, S., Torabi, S. A., & Mansouri, S. A. (2016). Humanitarian logistics network design under mixed uncertainty. *European Journal of Operational Research, 250*(1), 239–250.

Tzeng, G.-H., Cheng, H.-J., & Huang, T. D. (2007). Multi-objective optimal planning for designing relief delivery systems. *Transportation Research Part E: Logistics and Transportation Review, 43*(6), 673–686.

Unicef (2017). Humanitarian drone corridor launched in malawi. August 23, 2017. Available from: https://www.unicef.org/stories/humanitarian-drone-corridor-launched-malawi [Accessed 5 September 2022].

Unicef (2018). Child given world's first drone-delivered vaccine in vanuatu - UNICEF. December 18, 2018. Available from: https://www.unicef.org/press-releases/child-given-worlds-first-drone-delivered-vaccine-vanuatu-unicef [Accessed 5 September 2022].

UPS (2017). UPS tests residential delivery via drone launched from atop package car. February 21, 2017. Available from: https://www.globenewswire.com/news-release/2017/02/21/925955/0/en/UPS-Tests-Residential-Delivery-Via-Drone-Launched-From-Atop-Package-Car.html [Accessed 5 September 2022].

Vincent, J. (2021). Self-flying drones are helping speed deliveries of COVID-19 vaccines in Ghana. March 9, 2021. Available from: https://www.theverge.com/2021/3/9/22320965/drone-delivery-vaccine-ghana-zipline-cold-chain-storage [Accessed 5 September 2022].

Volocopter (2021). Available from: https://www.volocopter.com/solutions/volodrone/ [Accessed 5 September 2022].

Wang, Z., & Sheu, J.-B. (2019). Vehicle routing problem with drones. *Transportation Research Part B: Methodological, 122*, 350–364.

Yang, M., Kumar, S., Wang, X., & Fry, M. J. (2021). Scenario-robust pre-disaster planning for multiple relief items. *Annals of Operations Research*, 1–26. https://doi.org/10.1007/s10479-021-04237-3.

Yang, Y., Yin, Y., Wang, D., Ignatius, J., Cheng, T., & Dhamotharan, L. (2023). Distributionally robust multi-period location-allocation with multiple resources and ca-

pacity levels in humanitarian logistics. *European Journal of Operational Research, 305*(3), 1042–1062.
Zeng, Y., Xu, J., & Zhang, R. (2019). Energy minimization for wireless communication with rotary-wing UAV. *IEEE Transactions on Wireless Communications, 18*(4), 2329–2345.
Zhang, G., Jia, N., Zhu, N., Adulyasak, Y., & Ma, S. (2023). Robust drone selective routing in humanitarian transportation network assessment. *European Journal of Operational Research, 305*(1), 400–428.
Zhu, T., Boyles, S. D., & Unnikrishnan, A. (2022). Two-stage robust facility location problem with drones. *Transportation Research Part C: Emerging Technologies, 137*, 103563.
Zipline (2022). Global healthcare. Available from: https://www.flyzipline.com/global-healthcare/ [Accessed 5 September 2022].